

# OTDR-based optical fiber bending and tensile loss analysis\*

WANG Yang\*\*, WANG Xijun, and LI Xiaoling

Information Management Department, Northwest A&F University, Yangling 712100, China

(Received 1 September 2022; Revised 19 December 2022)

©Tianjin University of Technology 2023

When optical fiber is deployed in practical engineering, bending and stretching of fiber optics is inevitable, which will affect optical communication. The fiber losses of different bending radii are simulated by COMSOL software. In order to verify the accuracy of simulation results, an experiment was designed to measure the losses of single-mode fiber under different bending radii and tension forces. The results show that the sensitive bending diameter of fiber loss is between 5 mm and 10 mm. The tensile effect has little influence on the fiber loss, but when the tensile force is greater than 160 N, the fiber breaks. This study provides an important reference for fiber layout in practical engineering.

**Document code:** A **Article ID:** 1673-1905(2023)03-0164-6

**DOI** <https://doi.org/10.1007/s11801-023-2150-x>

In the 1960s, KONG<sup>[1]</sup> theoretically proved the possibility of using optical fiber as a transmission medium for realizing optical communication and predicted the possibility of manufacturing ultra low power optical fiber for communication. The rapid development of society has led to an increasing application of optical fiber technology, and researchers are paying increasing attention to the study of optical fiber loss. SHAHA et al<sup>[2]</sup> explained the effects of cladding geometries on hollow core conjoined-tube negative curvature fibers and offered a modified negative curvature conjoined-tube fiber with appropriate positioning of an additional layer of D-shaped negative curvature joining the flat bar to reveal attractive performance compared to recent related existing fibers, and the results showed the potential of conjoined-tube hollow-core negative curvature fibers in optical communication systems. Subsequently, SHAHA et al<sup>[3]</sup> proposed an anti-resonance hollow fiber without nodes with nested mixed cladding components, and the distance from the central layer to the sheath capillary was not great. It has been shown that the limited loss is less than 0.003 dB/km in the passband range of 670 nm (0.90—1.57  $\mu\text{m}$ ). MOHD ARIF et al<sup>[4]</sup> studied the optical loss in a standard single-mode step-index fiber due to fiber bending at a wavelength of 1 550 nm, and the result showed that the elliptical-shaped flexural configuration produced more contrast loss than the sinusoidal-shaped configuration at flexion angles of 180° and 360°. ROMAN et al<sup>[5]</sup> performed experiments at different bending radii (from 12.5 mm to 0.9 mm) and compared the large bending

losses of standard single-mode fibers with high numerical aperture thin core fibers, to confirm that thin-core high numerical aperture fibers can be used for Rayleigh-based backscattering. LI et al<sup>[6]</sup> designed an experiment to measure the fiber loss spectrum based on the insertion method, and tested the loss of fibers at different wavelengths. The principle and influencing factors of fiber bending loss were then analyzed<sup>[7]</sup>, and the flexural strength and temperature sensing characteristics of the 5 km sensor structure were tested by the Brillouin optical time domain reflectometer (BOTDR) system. The results show that the sensor structure has good resistance to bending and the minimum radius of curvature is 1.25 mm. WU et al<sup>[8]</sup> measured the bending loss coefficient of the single-mode fiber to be 1 550 nm when wound 1 to 4 times under standard temperature, high temperature, high humidity, salt fog and vulcanization conditions, and tested the mechanical strength of the fiber by tensile method<sup>[9]</sup>. WANG et al<sup>[10]</sup> investigated the influence of structural parameters of optical fibers (number of air-gap layers in the coating, duty cycle and fillet diameter) on optical fiber loss. ZHANG et al<sup>[11]</sup> analyzed the transmission characteristics of single-mode fiber with different coating materials (acrylate and polyimide) in a thermal environment under high vacuum conditions. JIANG et al<sup>[12]</sup> prepared multi-mode  $\text{As}_2\text{S}_3$  calorimeter fibers with different diameters by the extrusion method, and measured the loss of the fiber under different radii of bending. LIAO et al<sup>[13]</sup> tested optical fiber loss characteristics by modifying the core material

\* This work has been supported by the Cernet Innovation Project (No.NGII20190624).

\*\* E-mail: 1527wangyang@nwfafu.edu.cn

of the optical fiber. PAN *et al.*<sup>[14]</sup> investigated two types of dissipative soliton resonance and noise-like pulsations, which have some application value in the fields of optical sensing and spectral measurement. SUHAIMI *et al.*<sup>[15]</sup> studied important transmission characteristics including confinement loss, effective material loss (EML) and core power fraction by using the finite element method in COMSOL multi-physical simulation software, and studied effective area, bending loss and dispersion characteristics. ZHU *et al.*<sup>[16]</sup> investigated the micro-bending optical loss caused by the encapsulation of sensing fiber into a sandwich glass fiber reinforced structure through experiments and simulations. The results have shown that the positioning of the fiber in the fiber reinforced structure of flat woven glass has a significant effect on the optical loss of micro-bending. WEI *et al.*<sup>[17]</sup> studied the fiber loss caused by annealing. This demonstrates that the loss of the fiber can be irreversibly reduced by multiple cycles of annealing at the temperature of 800 °C. CUI *et al.*<sup>[18]</sup> studied the influence of the fusion current on the fusion loss of fused standard single-mode fiber. They showed that the change in the fusion current caused a different degree of core switching and led to different splice loss noise due to diffusion. ZHANG *et al.*<sup>[19]</sup> designed a high sensitivity refractive index sensor using fiber optics and applied it to the detection of glucose. It was found to have good sensitivity and have a potential application prospect. CUI *et al.*<sup>[20]</sup> used the finite element simulation method to gain a better understanding of the flexural sensing characteristics of fiber Bragg gratings, which provided a benchmark for the design and processing of fiber-optic flexure sensors.

VOS viewer software was used to perform a similarity analysis of high-frequency terms in article titles and abstracts and to generate a keyword tagging map. Bibliometric analysis was performed in June 2022. This study conducted the following search of the Web of Science database: Topic (“Fiber bending loss”) and Topic (“Fiber tensile loss”) or Topic (“Fiber bending and stretching loss”) or Topic (“Fiber loss”) and Topic (“Stretch bending\*”). 194 documents were obtained initially.

Keywords co-occurrence analysis shows the most frequently used term in the research field of fiber tensile bending loss. Keywords co-occurrence diagram of fiber stretching bending loss (Fig.1) was generated by VOS viewer software. Each round node in the diagram represents a keyword, and multiple keywords are connected by lines. The larger the nodes are, the higher the frequency of keywords is. The closer the distance between the two keywords, the stronger the correlation. Keywords co-occurrence network shows four keyword clusters, representing different subject groups of fiber tensile bending loss research. Cluster I (blue) represents mechanical and thermodynamic properties of fiber. Cluster II (red) represents the stretching behavior of composite fibers. Cluster III (yellow) stands for fiber optic applications in concrete and mechanical properties testing.

Cluster IV (green) refers to optical fiber stability and strength.

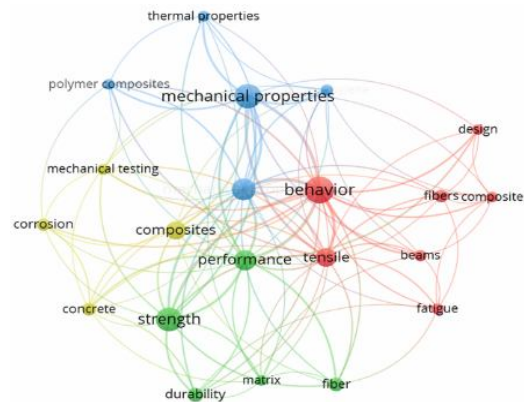


**Fig.1 Co-occurrence diagram of keywords fiber bending and stretching loss**

Although the aforementioned experiments are sufficient to examine the single factor influence of fiber loss, there are few researches that address the combined influence of bending and stretching on fiber loss, which may happen simultaneously in a practical fiber architecture. The optical fiber losses under various bending radii and tensile forces of straight pull are tested in this paper using an optical time domain reflectometer (OTDR) and the Rayleigh scattering principle. The optical fiber losses under various bending radii are compared and analyzed using the interpolation method, which has significant reference value for the optical fiber layout in actual engineering.

The three main scattering light spectra in optical fibers are Raman scattering light, Brillouin scattering light, and Rayleigh scattering light. In optical fiber temperature sensors, Raman scattering and Brillouin scattering are frequently utilized. The elastic light effect and the thermo-optical effect in the optical path cause the length and refractive index of the scattering element at the loss position to change when the connection point and breakpoint loss happen at a specific position of the optical fiber line, which results in the phase change of Rayleigh scattering light entering the optical fiber. Fiber loss is the term used to describe how optical fibers attenuate light wave power. The main component of fiber loss<sup>[21]</sup> is scattering loss, which also includes intrinsic loss, bending loss, docking loss, manufacturing loss, etc. Fiber attenuation coefficient, which may be stated as follows, is a common method for measuring fiber loss characteristics:

$$\hat{\alpha}_{(\lambda)} = \frac{10}{L} \lg\left(\frac{P_0}{P_1}\right), \quad (1)$$

where  $\hat{\alpha}_{(\lambda)}$  is the optical fiber attenuation coefficient, the wavelength is  $\lambda$ , the unit is dB/km, and  $L$  is the length of the optical fiber to be measured. What's more,  $L=2\pi R$ , and  $R$  is the bending radius of the optical fiber.

COMSOL simulation software has a clear interface, a strong ability to build and analyze models, an accurate

simulation environment, and fast computational speed. The finite element method described in this paper was used to numerically simulate single mode fiber bending loss, and COMSOL Multiphysics software version 5.6 was used to construct the fiber model, in order to accurately simulate and calculate the performance of the fiber in the real environment, including the mode field distribution, the effective refractive index, the bending loss, etc. A two-dimensional model was chosen to build the fiber core and cladding structure as well as the perfect matching layer, and the parameters were set to split the grid as illustrated in Fig.2.

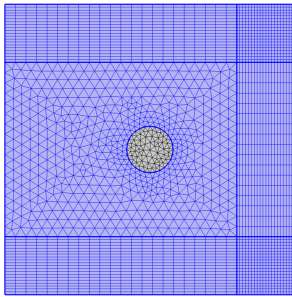


**Fig.2 Fiber optic grid division**

The fiber geometry and the difference in refractive index between the core and the cladding vary as a function of fiber curvature. Below, we show the equivalent refractive index of the fiber cross-section when the fiber is positively curved up the  $X$  axis<sup>[22]</sup>

$$n(x, y) = n_0(x, y) \sqrt{1 + 2x / R_{\text{eff}}}, \quad (2)$$

$$R_{\text{eff}} = 1.28R, \quad (3)$$

where  $n_0(x, y)$  represents the initial refractive index of the fiber without bending,  $R_{\text{eff}}$  represents the equivalent bending radius after the introduction of the elastic optical correction factor, and  $R$  represents the bending radius of the fiber.

According to Ref.[22], the formula for calculating fiber bending loss is as follows

$$\partial = -8.686 \frac{2\pi}{\lambda} \text{Im}(n_{\text{eff}}), \quad (4)$$

where  $\lambda$  represents the wavelength,  $\text{Im}$  represents the imaginary part, and  $n_{\text{eff}}$  is the effective refractive index of the fiber.

OTDR optical power meter is an optical fiber loss measurement instrument based on Rayleigh backscatter, which can determine the position of the optical fiber loss across the light-wave transmission time in the optical fiber<sup>[23,24]</sup>. The measurement range of the optical power meter is +7.00—70.00 dB. To ensure the accuracy of the data, the measurement would need to be within 2/3 of the measurement range, that is, +7.00—44.00 dB. In the national GB/T7424.2-2002 standard, two kinds of fiber tensile testing methods are given, namely, mandrel transfer, fiber wrap on mandrel, and pulley; the second is straight traction, and the optical fiber through the clamp-

ing device is fixed. Currently, the most commonly used type is a hand over type. ZHANG et al<sup>[25]</sup> tested fiber stretching based on the mandrel transfer type principle, and could calculate load, displacement, stress, and strain as well as other fiber stretch parameters. LU et al<sup>[26]</sup> proved the effectiveness of straight-pull fiber strain measurement by comparing the two measurement methods. The optical fiber bending loss is measured here by the OTDR based optical fiber sensor, and the fiber stretch loss is measured by a straight line traction. The equipment used in the experiment included Zeye-410T optical power meter, APM50 optical power meter, projectile force meter (0-200N), several monomode glass optical fibers (LC-SC), pliers, slideway, scale, several customized cylindrical molds with diameters of 5 mm to 40 mm (When the bending diameter is less than 5 mm, this will lead to inaccuracies due to the greatly increased optical fiber loss exceeding 2/3 of the optical power meter range, therefore, bending diameters less than 5 mm are not considered in this paper) and multiple gaskets. The disadvantages of bare fiber are that it will cause leakage of light. In addition, if there is a stain attached to the fiber, it will also cause light leakage<sup>[27]</sup>, which will introduce a large error into the experiment. For this reason, optical fiber with enclosing wire is selected in the experiment in this paper. The experimental layout is shown in Fig.3. The Zeye-410t optical power meter is used as the emitting light source to emit light with a wavelength of 1 550 nm. The APM50 optical power meter is set to receive light source in 1 550 nm mode, as shown in Fig.4. To avoid damage to the optical fiber, the gasket is bonded to the bonding location of the optical fiber during the clamping process. While the other end of the optical fiber is attached to the pulley track, and the projectile force meter is hung on the track and an increasing tensile force of 10 N is applied upwards on the opposite side of the level with the optical fiber. A scale is used to measure the slideway displacement and read off the corresponding tensile fiber loss. To measure the sensitivity of the bending loss of the fiber to the winding radius, the fiber was wound on to the cylinder with diameters of 5 mm, 10 mm, 20 mm, and 40 mm, respectively. Based on this, the fiber was wound on to a cylinder with a diameter of 8 mm for one turn in order to investigate the sensitivity of the tensile loss of the fiber to fiber curvature.



**Fig.3 Layout of straight-pull fiber tensile test**



**Fig.4 Optical power meter**

According to the theoretical fracture strength of optical fiber<sup>[28]</sup>, the fiber strength  $\sigma$  is inversely proportional to the square root of the crack size  $c$ . According to Griffith fracture theory, the expression is

$$\sigma = \sqrt{\frac{E\gamma}{c}}, \tag{5}$$

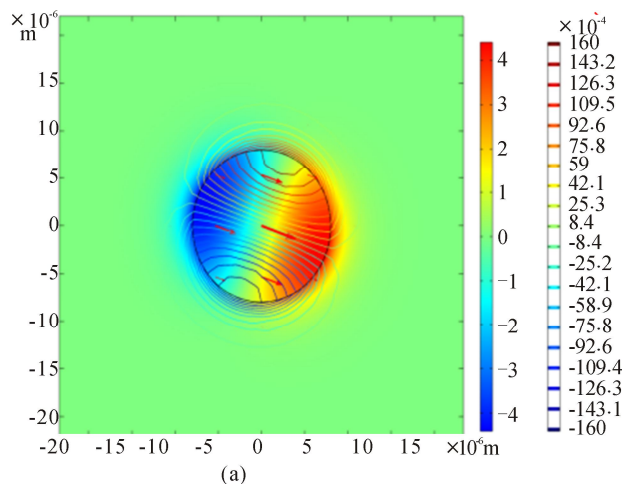
where  $E$  is the Young's modulus of the optical fiber, and  $\gamma$  is the surface energy of the sample.

$$\sigma = \frac{F}{S}. \tag{6}$$

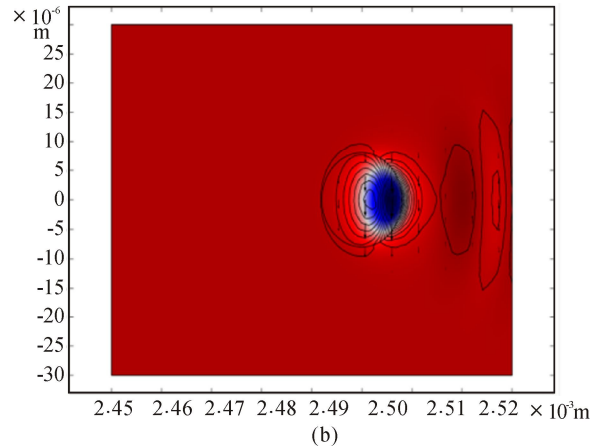
Suppose  $E=72.2$  GPa,  $\gamma=7 \times 10^{-5}$  kg/mm<sup>2</sup>,  $c=2 \times 10^{-7}$  mm, and substitute it into Eqs.(5) and (6) to get  $F=203$  N<sup>[9]</sup>.

The radius of the fiber core is 5  $\mu\text{m}$ , the cladding radius is 62.5  $\mu\text{m}$ , the thickness of perfect matching layer is 10  $\mu\text{m}$ , the refractive index of the fiber core is 1.445 7, the refractive index of the cladding is 1.437 8, and the wavelength is 1 550 nm. As the imaginary part of the effective index of refraction is 0 when the radius of curvature is less than 10 mm, simulations are only performed for the electric field plots with the radius of curvature of 15 mm, 20 mm, 25 mm, and 30 mm. The non-bending electric field pattern and the 15 mm radius of curvature are shown in Fig.5. In order to obtain the effective refractive indexes under different radii of curvature, Fig.6 shows that the corresponding bending loss is obtained according to Eq.(3).

To determine the sensitivity of fiber loss to wrap radius in this experimental environment, this study selected



(a)



(b)

**Fig.5 Electric field diagrams: (a) Non-bending optical fiber; (b) Bending optical fibers with a radius of 15 mm**

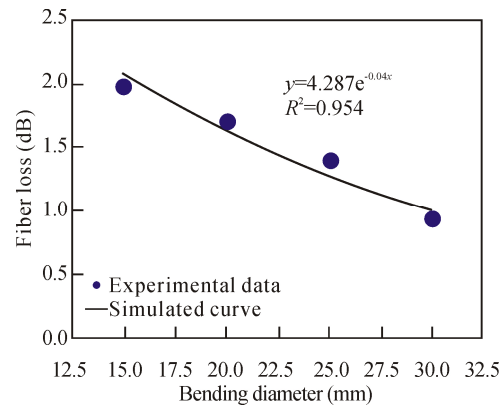


**Fig.6 Optical fiber loss simulation results with different bending radii**

cylinders of 5 mm, 10 mm, 20 mm, and 40 mm, and wrapped the fiber around the cylinder for a single turn in order to measure the fiber loss. Fig.7 shows the experimental results.

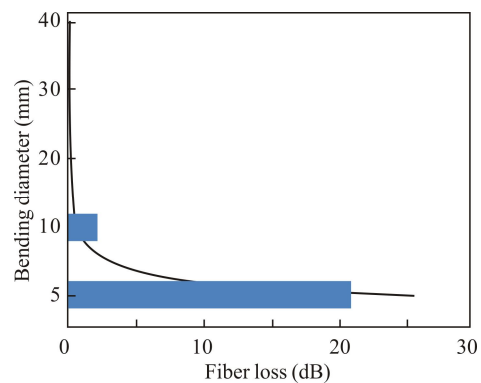


**Fig.7 Relationship model of fiber bending loss**

As shown in Fig.7, the fiber loss and bending diameter have a power function relationship, and the correlation coefficient is 0.93, which indicates high accuracy. With a bending diameter of 5—10 mm, the loss of the fiber changes significantly, the range of variation is approximately 2—20 dB, and it is consistent with the changing

trend in Fig.6, indicating that the simulation results are accurate. At bending diameters greater than 20 mm, fiber loss changes very little, nearly 0. For this reason, when conducting the fiber tension experiment, the winding diameter was chosen to be 8 mm, and the interpolation algorithm was used to find that the fiber loss was approximately 4.3 dB when the winding diameter was 8 mm.

As can be seen from Fig.8, with the increase of tensile force, the loss of optical fiber barely changes, and the slight rise is due to the slight bending of the initial optical fiber. As the pulling force is increased, the optical fiber is gradually elongated into a horizontal straight line, and the optical fiber loss is slightly decreased. On the other hand, when the pulling force is greater than 120 N, the optical fiber loss increases sharply. At a pulling force of 160 N, a "bang" noise is heard. If the optical fiber loss is greater than  $-44$  dB, which exceeds the threshold value, the optical fiber is considered to be broken. In Loss 2, when the pulling force is 140 N, the loss of the optical fiber exceeds the threshold value, which is related to the flaws in the chosen optical fiber. The average winding loss of the fiber in a single turn is  $-5.41$  dB higher than that with no winding, which is very close to the flexural loss of  $-4.3$  dB measured by the interpolation method, which fully tests the reliability of the experimental results.

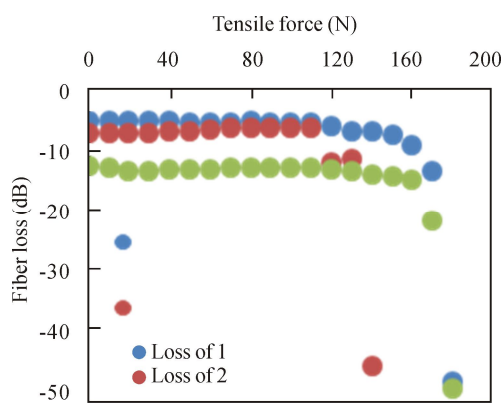


**Fig.8 Relationship model of fiber tensile loss**

By comparing Fig.7 and Fig.8, within a certain bending radius, fiber loss caused by fiber bending is much larger than the fiber loss caused by fiber stretching, which fully confirms that the fiber loss is more sensitive when the bending diameter is 5—10 mm.

Based on the principle of OTDR, Rayleigh scattering light was used to design fiber loss experiments under different bending radii and different tensile forces. The sensitivity of fiber to bending radius and tensile force was compared and analyzed. It was found that when bending diameter was from 5 mm to 10 mm, fiber loss was obvious, up to 20 dB. When the tensile force is small, the fiber loss is very small. When the tensile force is greater than 120 N, the fiber loss increases sharply until the fiber breaks when the tensile force is 160 N, and the

fiber loss exceeds the threshold. The fiber is more sensitive to bending radius (5—10 mm) than to fiber stretching. In practical engineering, optical fibers are inevitably stretched and bent. The results of this study provide a theoretical benchmark for minimizing optical fiber loss and avoiding damage during fiber optics.

### Statements and Declarations

The authors declare that there are no conflicts of interest related to this article.

### References

- [1] KONG D P. Research on key technologies of design, fabrication and application of micro-structured optical components[D]. Beijing: Graduate University of Chinese Academy of Sciences, 2013.
- [2] SHAHA K S R, KHALEQUE A. Low-loss single-mode modified conjoined tube hollow-core fiber[J]. Applied optics, 2021, 60(21): 6243-6250.
- [3] SHAHA K S R, KHALEQUE A, HOSEN M S. Wide-band low loss hollow core fiber with nested hybrid cladding elements[J]. Journal of lightwave technology, 2021, 39(20): 6585-6591.
- [4] MOHD ARIF N A A, BURHANUDDIN D D, SHAARI S, et al. Bend loss fiber optics design based on sinusoidal and ellipse configurations[J]. Optica applicata, 2021, 51(3).
- [5] ROMAN M, ZHU C, O'Malley R J, et al. Distributed fiber-optic sensing with low bending loss based on thin-core fiber[J]. IEEE sensors journal, 2021, 21(6): 7672-7680.
- [6] LI Y Q, LIU Y R, WANG L, et al. Design of experimental system for measurement of fiber loss spectrum[J]. Experimental technology and management, 2020, 37(5): 173-175.
- [7] LI Y Q, FAN H, WANG L, et al. Bend-tolerant fiber sensor based on BOTDR system[J]. Optoelectronics letters, 2022, 18(6): 343-348.
- [8] WU C, XU L X, ZHANG X M. Study on the variation of optical fiber bending loss coefficient with environment[J]. Journal of quantum electronics, 2018, 35(6): 752-758.
- [9] WU C. Study on mechanical strength and bending loss of optical fiber with environmental changes[D]. Heifei: University of Science and Technology of China, 2018.
- [10] WANG X, LOU S Q, XING Z. Loss characteristics of hollow core photonic band gap fiber[J]. Infrared and laser engineering, 2019, 48(S2): 103-108.
- [11] ZHANG J C, ZHANG W, YANG X N, et al. Study on transmission loss characteristics of optical fibers with different coatings under vacuum thermal environment[J]. Infrared and laser engineering, 2019, 48(11): 1-8.
- [12] JIANG L, DAI S X, LIU Y X, et al. Bending characteristics of As<sub>2</sub>S<sub>3</sub> chalcogenide glass fiber and its influence on loss[J]. Journal of silicate, 2019, 47(2): 250-254.
- [13] LIAO F X, WANG X S, NIE Q H, et al. Fabrication and

- properties of low-loss Ge-Te-Se core-clad fiber based on extrusion technology[J]. *Acta photonica sinica*, 2015, 44(10): 88-93.
- [14] PAN Y Z, QIU H X, ZHANG T Q, et al. Dissipative soliton resonance and noise-like pulse generation of large normal dispersion Yb-doped fiber laser[J]. *Optica applicata*, 2022, 52(1).
- [15] SUHAIMI N A N B, MAIDI A M, ABAS P E, et al. Design and simulation of heptagonal porous core photonic crystal fiber for terahertz wave transmission[J]. *Optik*, 2022, 260: 169142.
- [16] ZHU P, LIU P, WANG Z, et al. Evaluating and minimizing induced microbending losses in optical fiber sensors embedded into glass-fiber composites[J]. *Journal of lightwave technology*, 2021, 39(22): 7315-7325.
- [17] WEI S, LU M, LUO Y, et al. Annealing effects on optical losses in 3D-printed silica fiber[J]. *IEEE photonics technology letters*, 2022, 34(4): 199-202.
- [18] CUI Z, YUAN C. The effect of fusion current on thermally diffused expanded core of splicing ultra-low loss fiber and traditional single-mode fiber[J]. *Optical fiber technology*, 2021, 63: 102477.
- [19] ZHANG A, LI Y, PAN F, et al. High sensitivity SPR refractive index sensor with high resolution based on anti-resonance fiber[J]. *Optoelectronics letters*, 2022, 18(4): 0204-0209.
- [20] CUI W, ZHOU Y, YAN Z, et al. Simulation and experimental verification of off-axis fiber Bragg grating bending sensor with high refractive index modulation[J]. *Optoelectronics letters*, 2022, 18(4): 0200-0203.
- [21] WANG W M, SHI C Y, DASTAN Z. Intelligent contract experimental platform based on block chain technology[J]. *Experiment technology and management*, 2019, 36(3): 86-91.
- [22] JIN W X et al. Strict dual-mode large-mode-area fiber with multicore structure[J]. *Optics communications*, 2016, 366: 308-313.
- [23] WAN K T, LEUNG C Y. Applications of a distributed fiber optic crack sensor for concrete structures[J]. *Sensors and actuators A: physical*, 2007, 135(2): 458-464.
- [24] ZHAO Z. *Optical fiber communication engineering: communication engineering series*[M]. Beijing: Beijing Posts and Telecommunications Press, 2001.
- [25] ZHANG C F, FU K, MA B J, et al. Wheel wound optical cable tensile testing device[J]. *Machine tools and hydraulics*, 2017, 45(1): 92-95.
- [26] LU J L, ZHANG X M. Optical cable direct pull tensile test device based on BOTDR[J]. *Optical fiber and cable and its application technology*, 2005, (2): 17-19.
- [27] WANG S. Research on optical fiber loss detection technology for optical communication infrastructure construction [D]. Changchun: Jilin University, 2018.
- [28] GLAESEMANN G S. Advancements in mechanical strength and reliability of optical fibers[J]. *Reliability of optical fibers and optical fiber systems: a critical review*, SPIE, 1999, 10295(9): 5-27.